






Open Archive TOULOUSE Archive Ouverte (OATAO)

OATAO is an open access repository that collects the work of some Toulouse researchers and makes it freely available over the web where possible.

This is an author's version published in : <http://oatao.univ-toulouse.fr/9765>

Official URL : <https://dx.doi.org/10.1016/j.powtec.2013.08.008>

To cite this version :

Tourbin, Mallorie  and Al-Kattan, Ahmed  and Drouet, Christophe 
Study on the stability of suspensions based on biomimetic apatites aimed at biomedical applications, (2014) Powder Technology vol. 255 pp. 17-22.
ISSN 0032-5910

Any correspondence concerning this service should be sent to the repository administrator :
tech-oatao@listes-diff.inp-toulouse.fr

Study on the stability of suspensions based on biomimetic apatites aimed at biomedical applications

M. Tourbin ^{a,*}, A. Al-Kattan ^b, C. Drouet ^b

^a LGC (Laboratoire de Génie Chimique), UMR CNRS/INPT/UPS 5503; Université de Toulouse; 4 allée Emile Monso, 31432 Toulouse cedex 4, France

^b CIRIMAT Carnot Institute, UMR CNRS/INPT/UPS 5085; Université de Toulouse; Ensiacet, 4 allée Emile Monso, 31030 Toulouse cedex 4, France

ARTICLE INFO

Keywords:

Colloids
Nanocrystalline apatite
Stability
Biomedical applications
Characterization

ABSTRACT

Nanobiotechnologies have lately attracted much attention, both from therapeutic and diagnosis perspectives. In this view, the development of colloidal formulations of biocompatible nanoparticles capable of interacting with selected cells or tissues raises a particular interest, especially in link with cell-based pathologies such as cancer. In this context, the follow-up of colloidal stability and other physico-chemical features is of foremost relevance. In this contribution, we have focused our study on hybrid colloids based on biomimetic nanocrystalline apatites (analogous to those found in bone mineral) stabilized by adsorption of 2-aminoethylphosphate (AEP) molecules; these nanoparticles being intended to interact with cancer cells either for medical imaging (by conferring luminescence features to the apatite phase) or for therapeutic purposes. We show that various physico-chemical characteristics of the suspensions vary with time, including viscosity and mean particle size, suggesting a progressive structuration of the suspensions. Similar modifications were also noticed during the purification by dialysis. Finally, we report on preliminary experiments aimed at drying the colloids while retaining their capacity to recover their initial state after re-immersion in aqueous medium; so as to enable extended storage periods for the nanoparticles in their dry state while allowing their re-suspension at the time of use. On this matter, the addition of glucose prior to freeze-drying was found to be an effective way to avoid the formation of aggregates during drying.

This contribution thus confers additional information relative to the stability of AEP-stabilized biomimetic apatite colloidal formulations, which proved in previous studies to be of particular relevance for nanomedicine.

1. Introduction

This last decade has witnessed tremendous efforts aimed at developing innovative nanosystems (often formulated as colloids) capable of interacting with cells and tissues [1–5]. Such systems are especially relevant in the case of cancer pathologies in order to improve the efficacy of cancer treatments while significantly reducing side effects (therapeutic objectives), and also to facilitate early diagnosis therefore limiting cancer-related mortality (diagnosis objectives, e.g., through medical imaging). In the field of cancer diagnosis in particular, detection techniques based on luminescent nanoprobe exhibiting a specific affinity for some diseased cells have particularly raised interest in the view of tumor detection. Many systems of nanoprobe have been considered to-date for such medical imaging abilities, including in particular organic dyes such as green fluorescence protein or DAPI [6] or semiconductor quantum dots [7–9], among others. However, toxicity [10,11], photo-bleaching or flickering effects [12,13] are common limitations to these

systems which are thus not particularly suitable for the analysis of biological tissues, especially over extended periods of time. In this context, alternative nanosystems are being investigated, such as lanthanide-doped inorganic nanoparticles which are characterized by narrow emission bandwidths, high photochemical stability and long fluorescence lifetime (up to several milliseconds).

In this view, luminescent colloidal systems based on biomimetic calcium phosphate apatite nanoparticles (similar to bone mineral nanocrystals [14]) have been synthesized by soft chemistry [15], where the luminescence was conferred by substituting some calcium ions (a few atomic %) by rare-earth elements such as europium or terbium [16]. The idea to use biomimetic apatite particles as colloidal nanocarriers or nanoprobe is indeed particularly appealing taking into account the high biocompatible character of such apatites that are already present in Human's organisms in bones and teeth. In such nanocrystalline apatite-based systems, the colloidal-like character was linked to the adsorption [17], on the surface of apatite nanocrystals, of AEP molecules (2-aminoethylphosphate, a phospholipid moiety [18]) producing electrostatic repulsive effects between neighboring nanoparticles, thus hindering their aggregation. In previous works [15,19], the synthesis and main physico-chemical characteristics of such

colloidal nanoparticles (size, morphology, composition and luminescence properties) were investigated, and perspectives in terms of biological evaluations were commented. For example, the possibility to target cancer cells thanks to such apatite-based colloids has been illustrated very recently with the example of breast cancer cells and folic-acid functionalized apatite nanoparticles [16]. Monoclonal antibodies have also been shown to allow cell targeting approaches [20].

The efficacy of a purification of such apatite-based hybrid suspensions by dialysis process was also followed [19], this process being used to efficiently eliminate unreacted chemical species. However, macroscopic changes of the suspension state during this dialysis process were noticed (but not investigated in detail), resulting in particular in a more viscous system requiring a subsequent re-suspension treatment.

Taking these considerations into account, we followed in the present contribution various physico-chemical features of (non-luminescent) apatite-based suspensions, either before or after purification by dialysis, so as to better understand their physical state and appreciate their stability behavior.

Based on our results, drying and re-suspension aspects were also examined. Indeed, generally speaking, despite the advantages of drug delivery systems or imaging nanoprobe, several works have reported various potential issues linked to the manipulation of suspensions, including complex manufacturing, potential added toxicity due to the “nano” character of the carriers, and metastability [21–23]. Stability is indeed one of the critical aspects to take into account for ensuring safety and efficiency of systems used in nanomedicine. The colloidal stability may be affected by various factors such as the nature of the carrier and of the drug, its dose, the dispersion medium, the delivery route (e.g., intravenous, oral, intratumoral, etc.), and of course by production protocols. Stability issues associated with “nanosuspensions” have been widely investigated and can be subcategorized as “physical” and “chemical” stability. Common physical stability issues include in particular sedimentation/creaming effects, agglomeration, uncontrolled crystal growth and change of crystallinity state and can also affect the integrity of the drug or its mode of association with the nanocarrier (e.g., depending on storage and/or transportation conditions). Indeed, the large surface area of nanoparticles creates high total surface energy, which is thermodynamically unfavorable, tending to promote particle agglomeration so as to minimize the surface energy. The most common strategy to tackle this issue is to introduce stabilizers to the formulation. However, the stabilizer selection is known to be very challenging, and in addition to safety and regulation considerations, the selection of stabilizers is based on their ability to provide wetting to surface of the particles and offer a barrier to prevent nanoparticles from agglomeration [24,25]. Thus, the stability of nanoparticles used in nanomedicine formulations remains a very challenging issue during pharmaceutical developments.

In order to achieve preparations with shelf life of several years, water elimination from aqueous dispersions to obtain a dry solid form appears as the most promising strategy [26]. Freeze-drying technique has already found applications in the preparation of pharmaceutical powders with specific characteristics such as controlled particle size and shape.

The drying process may however be accompanied by an irreversible agglomeration of adjacent nanoparticles, thus potentially hindering further re-dispersion in solution prior to clinical use. The deagglomeration of the clusters could result of different chemical, hydrodynamic and mechanical mechanisms. When the forces causing deformation of the agglomerates exceed the cohesive forces due to interparticle binding, then agglomerates are expected to break-up into smaller fragments [27]. Several studies have pointed out that the kinetics of deagglomeration of nanoparticles-based powder and the morphology and rheology of the resulting suspensions strongly depend on physico-chemicals parameters such as pH for example [28–30]. Another objective of this work was thus to investigate also drying and re-dispersion processes, and to find a way to release the primary nanoparticles without major changes in their physico-chemical characteristics.

2. Materials and methods

2.1. Preparation of biomimetic apatite-based colloids

Apatite-based colloids were obtained by coprecipitation at room temperature of calcium nitrate and ammonium hydrogen phosphate in deionized water, at pH 9.5, in the presence of 2-aminoethylphosphate or “AEP”. The precipitates were then allowed to mature in an oven at 100 °C for 16 h. The starting AEP/Ca molar ratio was set to 1. For each preparation (25 ml), three aqueous solutions were prepared: solution (A), 6.25 ml, containing 4.87 mmol of calcium nitrate ($\text{Ca}(\text{NO}_3)_2 \cdot 4\text{H}_2\text{O}$), solution (B), 6.25 ml, containing 4.87 mmol of AEP, and solution (C), 12.5 ml, containing 1.62 mmol of ammonium hydrogenphosphate. Solution (A) was mixed with solution (B) under constant stirring. The acidic pH of the resulting solution as well as that of solution (C) were re-adjusted to 9.5 by addition of ammonia.

2.2. Purification by dialysis process

In this study, a tubular cellulose membrane (length: 15 cm, diameter: 3 cm, cutoff: 6000–8000 Da) was used as dialysis membrane, containing 25 ml of the suspension to dialyze. The membrane was held vertically and introduced in 800 ml of dialysis medium (deionized water). The washing medium was continually homogenized by mechanical stirring, and regularly exchanged by a fresh one (changes after 4, 8, 22 and 26 h of dialysis) so as to regenerate the concentration gradient and accelerate the purification process. The dialysis process was carried out at room temperature (25 °C).

When mentioned in the text, reagent grade sodium hexameta-phosphate (denoted here “HMP”) was added on the colloids after purification by dialysis in view of optimal particle dispersion. Typically, 1 ml of HMP aqueous solution at 0.08 M were added to 12.5 ml of the colloidal suspension.

2.3. Freeze-drying and redispersion

The suspensions were dried by freeze-drying. When mentioned in the text, glucose was added to the medium (150 mg of glucose added to 13.5 ml suspension, composed of 12.5 ml of colloid and 1 ml of HMP solution at 0.08 M) prior to the freeze-drying step. This biocompatible molecule was selected in view of forming, upon freeze-drying, a water-soluble solid matrix hindering the agglomeration of adjacent nanoparticles (as is generally noticed during water elimination from aqueous suspensions). The dry composite apatite/glucose agglomerates thus formed upon drying were then allowed to be redispersed in water, under moderate magnetic stirring (about 300 rpm).

2.4. Physico-chemical characterizations

The crystallographic structure of the powders obtained after freeze-drying the suspensions was investigated by way of X-ray diffraction (XRD) using a CPS 120 INEL diffractometer with the $\text{K}\alpha_1$ Cobalt radiation (1.78892 Å). For complementary analyses, Fourier transform infrared (FTIR) spectroscopy analyses were performed on a Nicolet 5700 spectrometer, in the wavenumber range 400–4000 cm^{-1} (resolution 4 cm^{-1}).

The calcium content of the nanoparticles was determined by induced coupled plasma atomic emission spectroscopy, ICP-AES (relative uncertainty 3%). The amount of mineral phosphate (from apatite) was measured by colorimetry at $\lambda = 460$ nm, using the yellow phosphovanado-molybdenum complex [31] (relative uncertainty 0.5%). The AEP content associated to the colloidal nanoparticles after purification by dialysis (thus after removal of all nitrate counter-ions) was drawn from nitrogen microanalysis (relative uncertainty 0.4%).

The particle size distributions of the suspensions were characterized without any dilution by dynamic light scattering (DLS) using a Zetasizer

Nano ZS (Malvern Instruments Ltd), with a backscattered light ($\lambda = 630 \text{ nm}$, $\theta = 173^\circ$). Punctual zeta potential measurements based on electrophoresis of the particles were carried out on the same apparatus using an adapted U-shaped measurement cell. For zeta potential measurements, no dilution was performed and the suspensions were tested as-prepared (synthesis pH of 9.5) without modification of medium.

Measurements of the rheological properties of the suspensions were performed with an AR rheometer (TA Instruments) at 25°C . The suspensions were analyzed by simple shear measurements using a parallel geometry (gap 1 mm) with serrated plates (diameter 60 mm).

Statistical relevance for the particle size and rheology measurements was tested on the basis of quadruplicate experiments.

3. Results and discussion

3.1. Structural and compositional analyses

The suspensions prepared in this contribution by apatite precipitation in the presence of 2-aminoethylphosphate (AEP) and purified by dialysis were first characterized by XRD and FTIR analyses. Figs. 1 and 2, respectively, report an XRD pattern and an FTIR spectrum that are typical of such colloidal nanoparticles, and these data confirmed the apatitic nature of the particles (main XRD diffraction lines corresponding to hydroxyapatite, space group $P6_3/m$ (hexagonal), have been added on Fig. 1).

Chemical analyses, however, indicated that the Ca/P mole ratio of the apatite phase was close to 1.42 and thus significantly lower than the value (1.67) found for hydroxyapatite. This finding points out the nonstoichiometry of such an apatite phase (closer to bone-like apatite). The AEP/apatite ratio characteristic of the sample was equal to 0.80. On the basis of nitrogen titration via elemental analyses, this amount of AEP was found to correspond to 11 wt.% in the hybrid apatite/AEP system. The presence of AEP molecules associated with the apatite phase was confirmed (Fig. 2) by the presence of an absorption band at 754 cm^{-1} , which is characteristic of the P–O(C) vibration mode in systems such as $\text{Ca}(\text{AEP})_2$ where a close interaction between AEP molecules (exhibiting one global negative charge at the synthesis pH) and Ca^{2+} ions is involved, as was discussed in previous works [15,28].

3.2. Surface charge analyses and stability

Zeta potential values obtained with these suspensions were systematically found to be positive ($\zeta \approx +12 \text{ mV}$ at the synthesis pH of 9.5) despite some variability, that is in good agreement with the presence of adsorbed AEP molecules, exposing their ammonium $-\text{NH}_3^+$ end-groups toward the solution (while the phosphate end of the AEP molecule interacts with the Ca^{2+} ions [32]). It may, however, be noted that this zeta potential value remains quite low (in absolute value), which

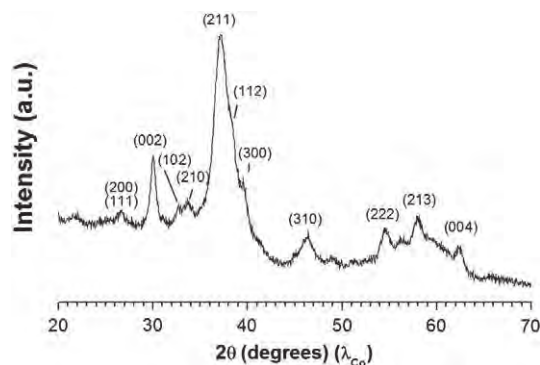


Fig. 1. XRD pattern for biomimetic apatite-based colloids stabilized by AEP molecules (prepared at 100°C , and pH 9.5), after dialysis purification.

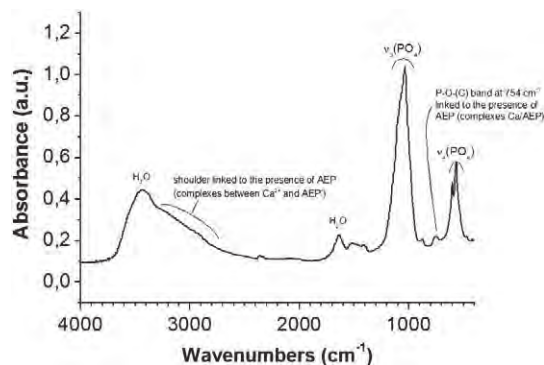


Fig. 2. FTIR spectrum for biomimetic apatite-based colloids stabilized by AEP molecules (prepared at 100°C , and pH 9.5), after dialysis purification.

thus does not enable us to describe such suspensions as highly stable, which is generally considered for absolute values above 30 mV.

3.3. Particle size characterizations

Optical observations (macroscopic), however, indicated that the as-synthesized colloids did not undergo sedimentation. DLS measurements on such as-prepared suspensions confirmed the nanometer-scale dimensions of the particles, with a unimodal size distribution centered around 30 nm. In order to inspect further the stability of these colloids, additional DLS measurements were carried out 1, 4, 7 and 15 days after synthesis (Fig. 3). In all cases, the mean hydrodynamic diameter was found to remain close to 30–35 nm. Interestingly, although a slight increase in mean particle size towards 35 nm was noticed here, no significant change could be seen over a period of 2 weeks after synthesis.

3.4. Rheological behavior of the suspensions

Rheological characterization showed that the suspensions had a rheofluidifying behavior, witnessed by a (nearly exponential) decrease of the suspension viscosity upon increase of the shear rate: in the range 0.1 to 0.001 Pa.s for shear rates varying from 0 and 300 s^{-1} . However, the viscosity of the suspensions was found to follow some evolutionary trend, increasing progressively upon ageing, which was followed over a period of 2 weeks. Moreover, a progressive increase of shear stress (see Fig. 4) was evidenced, tending towards a threshold value close to 0.1 Pa (starting value at zero shear rate) after few days of ageing. These results thus suggest that, although no sedimentation occurs, a progressive structuration of the suspension happens upon

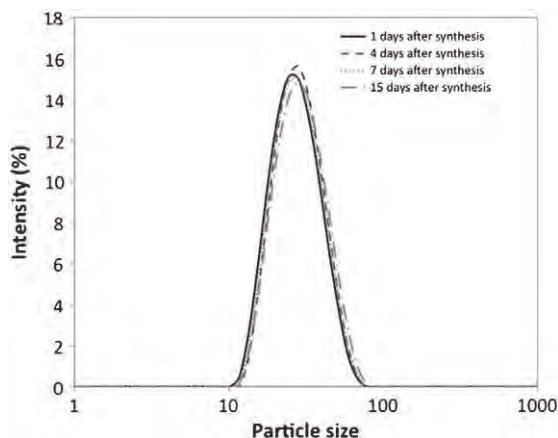


Fig. 3. DLS measurements versus time, for biomimetic apatite-based colloids stabilized by AEP molecules (prepared at 100°C , and pH 9.5).

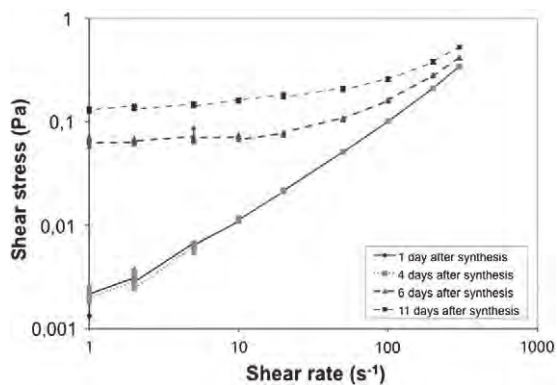


Fig. 4. Evolution of the rheograms of a nanocrystalline apatite suspension, as a function of ageing time after synthesis.

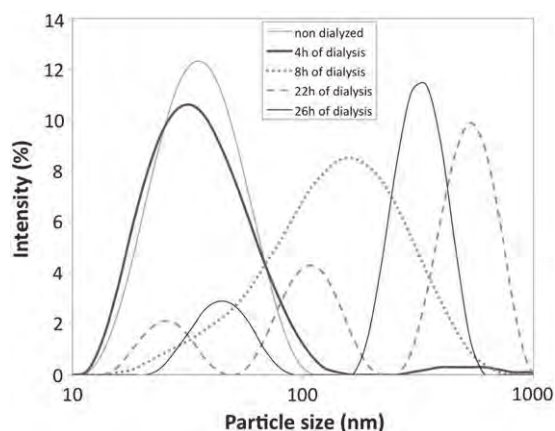


Fig. 5. Evolution of the particle size distribution during the dialysis process.

ageing, which underlines some limitations in the time-dependent stability of these suspensions.

3.5. Purification of the suspensions by dialysis

In a second step, the colloids stability was examined during the purification process of dialysis and analyses of the suspension were done for increasing durations of dialysis between 0 and 26 h of process. The follow-up of the particle size distributions versus time (Fig. 5) then pointed out a noticeable alteration in terms of particle size, marked by a global increase of the mean diameter of the particles and the appearance upon dialysis of new populations of aggregates around 100 nm and then 300–600 nm (Table 1). As it can be shown, the particle size distribution of the suspension quite remains the same after 4 h of dialysis. But after 8 h, aggregates of very different sizes have appeared and a large peak ($\sigma \approx 106$ nm) centered on medium aggregates sizes ($d_{2\text{peak}} \approx 153$ nm) can be observed. Then as the dialysis process goes

on, the particle size distributions highlight the existence of three populations: primary particles, and two populations of aggregates.

This size effect was accompanied by a progressive increase of the viscosity of the suspension during the dialysis process as shown in Fig. 6. During this type of size measurements, the auto-correlation function of each analysis also gives interesting information about the suspension and the quality of the results. Then the corresponding correlograms were verified too and they indicated the likely presence of larger particles or aggregates (larger than the upper limit of the apparatus which is over 6 μm), and of a significant polydispersity of the particles at this stage.

Although the rheofluidifying behavior of the suspension was conserved at all times during the dialysis process (Fig. 6), the increase in viscosity may be related to the above-mentioned increase of particle size, witnessing the evolution of the suspension structuration upon dialysis. In addition to possible dissolution–reprecipitation phenomena during the dialysis process, these effects may probably be linked to the desorption of some AEP molecules out of the surface of the apatite nanocrystals, therefore lowering the strength of electrostatic repulsive forces at the origin of the limitation of agglomeration. This is indeed supported by the fact that the relative intensity of the FTIR band at 754 cm^{-1} related to adsorbed AEP tends to decrease progressively as the dialysis process progresses (not shown here for the sake of brevity).

Very interestingly, we showed, however, that the addition of a dispersing agent involving multiple ionic end-groups, such as sodium hexametaphosphate, led to the recovery of a size closed to the mean particle size of the colloidal nanoparticles (as measured before dialysis), i.e., close to 40 nm (Fig. 7). After HMP addition, the observable refluidification effect was (as expected) accompanied by a quantitative decrease of the suspension viscosity, reaching the initial value obtained before dialysis (Fig. 6). The addition of HMP in the medium, which exhibits 6 negatively charged phosphate “heads,” is indeed likely to interact with the surface of the apatite nanoparticles covered with AEP molecules and presenting some peripheral positively charged amino groups. Such an interaction could then probably explain the refluidification effect observed, by an increased separation of adjacent nanoparticles, thus indicative of a re-individualization of the nanoparticles (destruction of the above-mentioned structuration of the suspension). Zeta potential measurements performed on such HMP-treated colloids indeed pointed out a change in sign of the nanoparticles in the presence of HMP molecules, typically reaching -16 mV [17]. Fig. 8 shows the typical morphology of nanoparticles obtained, after synthesis and HMP treatment, as observed by Transmission Electron Microscopy (TEM).

Taking into account the final objective of use of such colloids, the stability of such purified and HMP-redispersed suspensions was also checked in a preliminary way by subjecting them to the presence of (1) albumin (the main protein present in human plasma) at a concentration similar to that found *in vivo* (i.e. 43 g/l), (2) a solution of simulated body fluid (SBF) and (3) a mixture of the two. The colloidal stability was found to be retained at least for one week after such treatments without any detectable sign of agglomeration or sedimentation thus suggesting a possible use in contact with plasma.

Table 1
Characteristic diameters of the particle size distributions of the suspension during the dialysis process. $d_{i\text{peak}}$ (nm) is the mode of the peak i , σ (nm) the standard deviation of $d_{i\text{peak}}$ and Prop i (%) is the proportion of intensity of the mode of the peak i comparing to the other modes (Prop1 + Prop2 + Prop3 = 100%).

| | | Primary particles | | | Aggregates | | | Agglomerates | | |
|----------|-------------|-------------------------|-----------------|---------------|-------------------------|-----------------|---------------|-------------------------|-----------------|---------------|
| | | $d_{1\text{peak}}$ (nm) | σ_1 (nm) | Prop $_1$ (%) | $d_{2\text{peak}}$ (nm) | σ_2 (nm) | Prop $_2$ (%) | $d_{3\text{peak}}$ (nm) | σ_3 (nm) | Prop $_3$ (%) |
| Dialysis | Nondialyzed | 35 | 17 | 100 | | | | | | |
| | 4 h | 33 | 19 | 100 | | | | | | |
| | 8 h | | | | 153 | 106 | 100 | | | |
| | 22 h | 27 | 6 | 13 | 106 | 15 | 26 | 531 | 166 | 61 |
| | 26 h | 44 | 14 | 20 | | | | 319 | 89 | 80 |

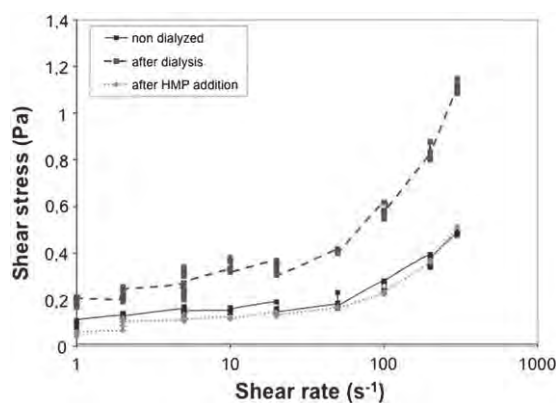


Fig. 6. Comparison of the rheograms for a nanocrystalline apatite suspension after synthesis (non dialyzed), then at the end of the dialysis process and finally after the HMP addition.

3.6. Drying and redispersion of the particles

The above findings indicate that some alterations of the suspensions physico-chemical properties, especially in terms of viscosity and/or mean particle size, could be noticed and followed upon ageing and/or during the dialysis purification process itself. It was thus interesting at this point to attempt to dry such suspensions (in view of significantly facilitating their storage over extended periods of time) while retaining an ability to be re-suspended in aqueous medium without significant change in particle size. First drying experiments carried out either in a drying oven or by direct freeze-drying were unsuccessful as they led to noticeably agglomerated particles in a rather irreversible way, which was evidenced by a sedimentation of part of the particles, even upon sonication. These findings may probably be linked to the high surface energy of apatite nanocrystals which are prone to interact strongly with each other, upon elimination of water, in view of minimizing the total surface energy of the system [33]. In this context, preliminary experiments were then run by freeze-drying the suspensions after addition of glucose in the medium (150 mg in 13.5 ml suspension, composed of 12 ml of colloid and 1 ml of HMP solution at 0.08 M). The original underlying idea in the use of glucose here is in fact linked to its water solubility: glucose (if added in sufficient quantity) is indeed expected to form a solid matrix “embedding” the apatite nanoparticles, thus hindering their agglomeration upon drying; while re-immersion in water at the time of use will again liberate the nanoparticles by solubilization of the glucose “embedding” matrix. In this case, re-suspension was found to be successful as no sedimentation occurred and DLS experiments revealed that no major change in particle size was detected as compared to the initial suspension (mean hydrodynamic diameter

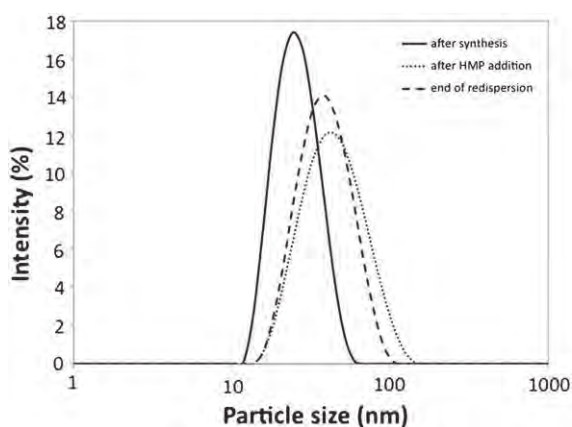


Fig. 7. Comparison of the particle size distribution on the suspension after synthesis, after dialysis and the HMP addition and at the end of the redispersion process.

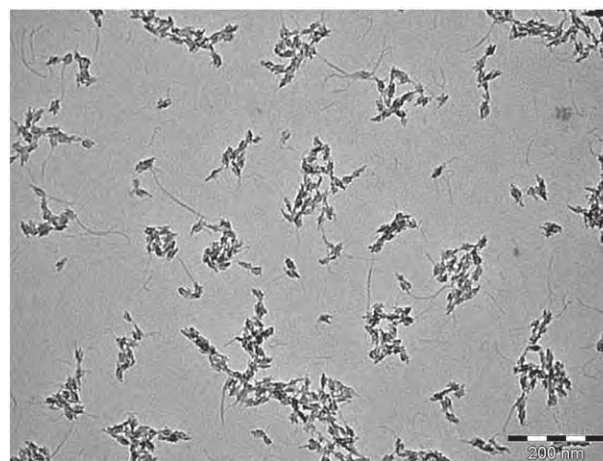


Fig. 8. Effect on particle size of an addition of HMP to the suspension.

close to 40 nm) (Fig. 7). Therefore, the colloidal behavior of the nanoparticles after redispersion was not affected. These results suggest that the addition of glucose into the system indeed formed the expected (water-soluble) matrix around the nanoparticles during the freeze-drying process, thus preventing their interaction/aggregation. After re-immersion, the solubilization of glucose then permitted to retrieve individual dispersed nanoparticles. These findings are thus promising in view of the storage over long periods of time of such colloids (under their dry state) for the setup of innovative injectable colloids for medical imaging or intracellular therapeutic applications.

For gaining additional insight on the behavior of such dried suspensions during re-immersion processes, redispersion experiments were done with varying volumes (thus leading to different conditions of particle concentrations). The dilution factor, f , was varied between 0.5 and 4 (f being the ratio between the volume of the suspension after redispersion and the volume of the suspension before freeze-drying). The evolution of the particle size distributions was characterized by DLS during the redispersion process and kinetics of redispersion can be represented by the evolution of the particle mean diameter versus time as in Fig. 9. It can be concluded that whatever the concentration, a size close to the primary particles size is reached after about 30 min of agitation. The decrease in size is first very fast (about 5–10 min), then it still decreasing more slowly and there is a stabilization until about 30 min. Furthermore, the higher the dilution factor, the faster the redispersion.

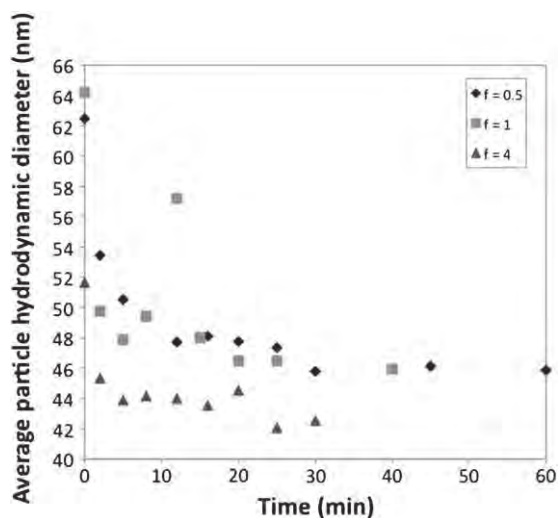


Fig. 9. Evolution of the particle mean hydrodynamic diameter during the dispersion process for three different dilution factors.

These findings thus indicate that it is possible to store such AEP-stabilized nanocrystalline apatite suspensions in a dry state, e.g., by addition of water-soluble glucose prior to the drying process, while preserving their ability to be redispersed in aqueous medium (and in varying concentrations) at the time of use. This statement is important in view of the possible use of such nanosuspensions in nanomedicine applications.

4. Concluding remarks

In this work, various physico-chemical features of colloidal-like suspensions formed of apatite nanoparticles functionalized by 2-aminoethylphosphate were examined. In particular, an evolution of the suspensions viscosity and/or mean particle size was evidenced upon ageing or during the purification process of dialysis, leading to their progressive structuration. The addition of a dispersing agent, in this case sodium hexametaphosphate, however, enabled us to efficiently re-suspend the nanoparticles after dialysis, and the addition of glucose (a water-soluble matrix-forming biocompatible molecule) allowed us to freeze-dry the suspensions while retaining their ability to be re-suspended, thanks to the formation of a glucose matrix around the particles during the drying process, thus hindering their agglomeration.

This contribution thus sheds some more light on the physico-chemistry and colloidal (meta)stability of suspensions prepared from biomimetic apatite/AEP hybrid compounds, thus unveiling potential limitations and interests of such biocompatible compounds intended for medical imaging or intracellular therapeutic applications.

Nomenclature

Latin letters

| | |
|--------------------|---|
| $d_{i\text{peak}}$ | mode of the peak i of the particle size distribution (nm) |
| f | dilution factor (—) |
| Prop i | proportion of intensity of the mode of the peak i (%) |

Greek letters

| | |
|-----------|-------------------------|
| λ | wave length (nm) |
| θ | scattering angle (°) |
| ζ | zêta potential (mV) |
| σ | standard deviation (nm) |

Acronyms

| | |
|---------|---|
| AEP | 2-aminoethylphosphate |
| DLS | dynamic light scattering |
| FTIR | Fourier transform distribution |
| HMP | hexametaphosphate |
| ICP-AES | induced coupled plasma atomic emission spectroscopy |
| TEM | transmission electron microscopy |
| XRD | X-ray diffraction |

Acknowledgements

Part of this work was financially supported by the Institut National Polytechnique de Toulouse (INPT) as BQR funding.

References

[1] Y. Lu, P.S. Low, Folate-mediated delivery of macromolecular anticancer therapeutic agents, *Adv. Drug Deliv. Rev.* 54 (2002) 675.
 [2] D. Pan, J.L. Turner, K.L. Wooly, Folic acid-conjugated nanostructured materials designed for cancer cell targeting, *Chem. Commun.* 19 (2003) 2400.

[3] X. Montet, K. Montet-Abou, F. Reynolds, R. Weissleder, L. Josephson, Nanoparticle imaging of integrins on tumor cells, *Neoplasia* 8 (2006) 214.
 [4] P. Chan, M. Kurisawa, J.E. Chung, Y. Yang, Synthesis and characterization of chitosan-g-poly(ethylene glycol)-folate as a non-viral carrier for tumor-targeted gene delivery, *Biomaterials* 28 (2007) 540.
 [5] S. Soppimath, L.H. Liu, W.Y. Seow, S.Q. Liu, R. Powell, P. Chan, Y.Y. Yang, Multifunctional core/shell nanoparticles self-assembled from pH-induced thermosensitive polymers for targeted intracellular anticancer drug delivery, *Adv. Funct. Mater.* 17 (2007) 355.
 [6] A. Miyawaki, Visualization of the spatial and temporal dynamics of intracellular signaling, *Dev. Cell* 4 (2003) 295.
 [7] M. Bruchez, M. Moronne, P. Gin, S. Weiss, A.P. Alivisatos, Semiconductor nanocrystals as fluorescent biological labels, *Science* 281 (1998) 2013.
 [8] W.J. Parak, D. Gerion, T. Pellegrino, D. Zanchet, C. Micheel, S.C. Williams, R. Boudreau, M.A. Le Gros, C.A. Larabel, A.P. Alivisatos, Biological applications of colloidal nanocrystals, *Nanotechnology* 14 (2003) R15.
 [9] F. Meiser, C. Cortez, F. Caruso, Biofunctionalization of fluorescent rare-earth-doped lanthanum phosphate colloidal nanoparticles, *Angew. Chem.* 43 (2004) 5954.
 [10] B. Ballou, B.C. Lagerholm, L.A. Ernst, M.P. Bruchez, A.S. Waggoner, Noninvasive imaging of quantum dots in mice, *Bioconjug. Chem.* 15 (2004) 79.
 [11] A.M. Derfus, W.C.W. Chan, S.N. Bhatia, Probing the cytotoxicity of semiconductor quantum dots, *Nano Lett.* 4 (2004) 11.
 [12] K.T. Shimizu, R.G. Neuhauser, C.A. Leatherdale, S.A. Empedocles, W.K. Woo, M.G. Bawendi, Blinking statistics in single semiconductor nanocrystal quantum dots, *Phys. Rev. B* 63 (2001) 205.
 [13] X. Brokmann, J.P. Hermier, G. Messin, P. Desbiolles, J.P. Bouchaud, M. Dahan, Statistical aging and nonergodicity in the fluorescence of single nanocrystal, *Phys. Rev. Lett.* 90 (2003) 120601.1.
 [14] R.Z. Legeros, in: B. Pamplin (Ed.), *Progress in Crystal Growth And Characterization Of Materials*, vol. 4, Pergamon Press, New York, 1981, pp. 1–45.
 [15] A. Al-Kattan, P. Dufour, J. Dexpert-Ghys, C. Drouet, Preparation and physicochemical characteristics of luminescent apatite-based colloids, *J. Phys. Chem. C* 114 (2010) 2918.
 [16] A. Al-Kattan, V. Santran, P. Dufour, J. Dexpert-Ghys, C. Drouet, Novel contributions on luminescent apatite-based colloids intended for medical imaging, *J. Biomater. Appl.* (2013)(online pre-publish number 0885328212473510).
 [17] A. Al-Kattan, Développement de nano-systèmes hybrides à base d'apatites biomimétiques en vue d'applications biomédicales en cancérologie. (PhD thesis) INP Toulouse, France, 2010.
 [18] L. Rothfield, A. Finkelstein, *Membrane Biochemistry*, *Annu. Rev. Biochem.* 37 (1968) 463.
 [19] A. Al-Kattan, P. Dufour, C. Drouet, Purification of biomimetic apatite-based hybrid colloids intended for biomedical applications: a dialysis study, *Colloids Surf. B* 82 (2011) 378.
 [20] M. Iafisco, E. Varoni, M. Di Foggia, S. Pietronave, M. Fini, N. Roveri, L. Rimondini, M. Prat, Conjugation of hydroxyapatite nanocrystals with human immunoglobulin G for nanomedical applications, *Colloids Surf. B Biointerfaces* 90 (2012) 1–7.
 [21] W. Abdelwahed, G. Degobert, S. Stainmesse, H. Fessi, Freeze-drying of nanoparticles formulation, process and storage considerations, *Adv. Drug Deliv. Rev.* 58 (2006) 1688–1713.
 [22] J.E. Kipp, The role of solid nanoparticle technology in the parenteral delivery of poorly water-soluble drugs, *Int. J. Pharm.* 284 (2004) 109–122.
 [23] L. Wu, J. Zhang, W. Watanabe, Physical and chemical stability of drug nanoparticles, *Adv. Drug Deliv. Rev.* 63 (2011) 456–469.
 [24] L. Gao, D. Zhang, M. Chen, Drug nanocrystals for the formulation of poorly soluble drugs and its application as a potential drug delivery system, *J. Nanopart. Res.* 10 (2008) 845–862.
 [25] B.V. Eerdenbrugh, G.V.D. Mooter, P. Augustijns, Top-down production of drug nanocrystals: nanosuspension stabilization, miniaturization and transformation into solid products, *Int. J. Pharm.* 364 (2008) 64–75.
 [26] P. Tewa-Tagne, S. Briançon, H. Fessi, Preparation of redispersible dry nanocapsules by means of spray-drying: development and characterisation, *Eur. J. Pharm. Sci.* 30 (2007) 124–135.
 [27] L. Xie, C.D. Rielly, W. Eagles, G. Ozcan-Taskin, Dispersion of nano-particle clusters using mixed flow and high shear impellers in stirred tanks, *Chem. Eng. Res. Des.* 85 (2007) 676–684.
 [28] L. Hui, P. Xueman, X. Mingxia, X. Tingxian, Dispersion mechanisms of aqueous silicon nitride suspensions at high solid loading, *Mater. Sci. Eng. A* 465 (2007) 13–21.
 [29] P. Ding, A.W. Pacek, Effect of pH on deagglomeration and rheology/morphology of aqueous suspensions of goethite nanopowder, *J. Colloid Interface Sci.* 325 (2008) 165–172.
 [30] M. Tourbin, C. Frances, Monitoring of the aggregation process of dense colloidal silica suspensions in a stirred tank by acoustic spectroscopy, *Powder Technol.* 190 (2009) 25–30.
 [31] G. Charlot, *Chimie Analytique Quantitative*, vol. 2, Masson, Paris, 1974, pp. 366–478.
 [32] A. Bouladjine, A. Al-Kattan, P. Dufour, C. Drouet, New advances in nanocrystalline apatite colloids intended for cellular drug delivery, *Langmuir* 25 (2009) 12256–12265.
 [33] S. Rollin-Martin, Développement de nouvelles biocéramiques par consolidation à basse température d'apatites nanocrystallines biomimétiques. (PhD Thesis) INP Toulouse, France, 2011.